N71-16528

NASA TECHNICAL MEMORANDUM

NASA TM X-52960

NASA TM X-52960

CASE FILE COPY

EFFECT OF RANDOM FLUCTUATIONS IN PRESSURE GRADIENT ON CHANNEL FLOW

by Morris Perlmutter
Lewis Research Center
Cleveland, Ohio

EFFECT OF RANDOM FLUCTUATIONS IN PRESSURE

GRADIENT ON CHANNEL FLOW

by Morris Perlmutter

Lewis Research Center
National Aeronautics and Space Administration
Cleveland, Ohio

ABSTRACT

A randomly fluctuating pressure gradient of a stationary Gaussian Markovian form will cause a randomly fluctuating velocity to be superimposed on the steady incompressible flow in a channel. Correlations, spectra, and frequency response functions for the random functions are given. Random pressure signals were generated using Fourier series expansion with coefficients randomly picked from distributions whose parameters were obtained from the spectra of pressure signal. The random velocity signals were then obtained from the pressure signal by use of the frequency response function calculated from the equation of motion. The increased power loss due to the fluctuations is given and the random pressure and velocity signals are compared for amplitude, frequency, and time lag.

INTRODUCTION

In many practical situations, flows in channels will have random pressure gradient fluctuations. It is of interest to understand the effect of the randomly fluctuating pressure gradient on the characteristics of the flow. The analysis is restricted to channel regions sufficiently downstream from the channel entrance so that entrance effects can be neglected. The analysis gives the mean square value of the velocity fluctuation across the channel as well as the increased power loss in pumping the fluid due to the fluctuations in the velocity.

A random sampling or Monte Carlo approach is also used, to generate a specific pressure gradient signal having a given power spectrum and a Gaussian distribution of amplitudes. This calculation can be rapidly carried out by use of fast Fourier transforms. The randomly varying pressure gradient signal generated is then used to find the corresponding fluctuating velocity signal at various positions across the channel. These numerical signal results can be useful, for instance, in numerical convective heat-transfer calculations in which numerical values for the randomly fluctuating velocity are required as input to calculate wall heat transfer.

SYMBOL

a_n, b_n	complex coefficients
d	spacing between parallel plates
f_o	frequency increment, $1/T_p$
f_p	maximum frequency
H	frequency response function
$\lvert H \rvert$	gain factor
h	weighting function or impulse response function
K	$k\pi$
N	number of samples
P	pressure gradient
R_{xy}	correlation $\langle x, y \rangle$
S	mean square power spectral density
T	time
T_p	period of record

t	dimensionless time, $\nu T/d^2$
Δt	time between sample
U	fluid velocity
u_s	steady dimensionless velocity, $-\nu\rho U_s/d^2 P_s$
v	transient dimensionless velocity, $-\nu\rho U_t/d^2 P_s$
Y	coordinate across channel
Y_K	4 sin Ky/K
y	dimensionless coordinate across channel, Y/d
γ	dimensionless pressure gradient, P_t/P_s
Λ	measure of rate of fluctuation of pressure signal
λ	dimensionless meassure of rate of fluctuation of pressure signal, $\Lambda d^2/\nu$
ν	kinematic viscosity
ρ	density
σ_γ^2	variance measure of pressure fluctuations
τ	dimensionless time difference, $t_2 - t_1$
φ	phase factor
ω	angular frequency, $2\pi f$
$\langle \rangle$	ensemble average
*	complex conjugate

Subscripts:

F	fundamental frequency or lowest frequency, $1/T_p$
H	related to frequency response function
I	imaginary
k	finite spatial sine transformed variable

R real

s steady component

t fluctuating component

γ related to pressure signal

ω Fourier time transformed variable

ANALYSIS

For viscous incompressible flow between parallel plates with constant properties in the fully developed flow region (see fig. 1) the momentum equation can be written as (ref. 1)

$$\partial U/\partial T = -1/\rho \; P(T) + \nu \; \partial^2 U/\partial Y^2 \tag{1}$$

We can let the velocity and the pressure gradient consist of a steady part and a nonsteady part

$$U = U_s + U_t; \quad P = P_s + P_t$$

Normalizing the variables as follows

$$u_s = -\nu\rho U_s/d^2 P \quad v = -\nu\rho U_t/d^2 P \quad y = Y/d \quad t = \nu T/d^2 \quad \gamma = P_t/P_s \tag{2}$$

we obtain for equation (1)

$$d^2 u_s/dy^2 = 1 \quad \text{or} \quad u_s = y - y^2/2; \quad \partial v/\partial t = \gamma + \partial^2 v/\partial y^2 \tag{3a;b}$$

Taking Fourier transforms of equation (6) we obtain

$$v_\omega i\omega = \gamma_\omega + \partial^2 v_\omega/\partial y^2 \tag{4}$$

Taking the finite sine transform of equation (4) gives

$$i\omega v_{\omega k} = 4\gamma_\omega/K - K^2 v_{\omega k}; \quad k = 1,3,5 \ldots \tag{5}$$

where $K = k\pi$. By solving for $v_{\omega k}$ and taking the inverse finite Fourier transform, we obtain

$$v_\omega = \gamma_\omega H \tag{6}$$

where

$$H = \sum_{k=1,3,5}^{\infty} Y_K/(K^2 + i\omega) = H_R + iH_I = |H| e^{-i\varphi_H} \tag{7}$$

where $Y_K = 4 \sin Ky/K$. The H is sometimes called the frequency response function, $|H|$ the gain factor, and φ_H the phase factor, where

$$|H|^2 = H_R^2 + H_I^2; \quad \varphi_H = \tan^{-1}(H_I/H_R) \tag{8;9}$$

The gain factor is plotted in figures 2 and 3; the phase factor is plotted in figure 2 and is discussed more fully later where used. We can solve equation (6) for v by taking the inverse transform. Using the convolution theorem gives

$$v = \int_{-\infty}^{+\infty} e^{i\omega t}\gamma_\omega H \, df = \int_{-\infty}^{+\infty} h(\theta,y)\gamma(t - \theta)d\theta \tag{10}$$

where h is the weighting function given by

$$h(\theta) = \int_{-\infty}^{+\infty} He^{i\omega\theta} \, df = \begin{cases} \displaystyle\sum_{k=1,3,5}^{\infty} Y_K e^{-K^2(\theta)} & \text{for } \theta > 0 \\ \\ 0 & \text{for } \theta > 0 \end{cases} \tag{11}$$

The h and H are a Fourier transform pair. Since the process is station-
ary, we can write the cross correlation equation as

$$\langle \gamma(t_1) v(t_1 + \tau) \rangle = R_{\gamma v}(\tau) = \int_0^\infty h(\theta, y) R_{\gamma\gamma}(\tau - \theta) d\theta \tag{12}$$

where $t_2 - t_1 = \tau$. Since the cross spectrum is the Fourier transform of the
cross correlation, by using the convolution theorem as before, we can write.

$$S_{\gamma v}(\omega) = H(\omega) S_{\gamma\gamma}(\omega) \tag{13}$$

We can find the velocity autocorrelation as

$$R_{vv}(\tau) = \int_0^\infty h(\theta, y) R_{\gamma v}(\tau + \theta) d\theta \tag{14}$$

We can then write the velocity power spectrum as

$$S_{vv}(\omega) = |H(\omega)|^2 S_{\gamma\gamma}(\omega) \tag{15}$$

This shows the velocity spectrum is equal to the pressure spectrum
times the square of the gain factor.

Pressure Gradient Correlations and Power Spectrum

A common form of random fluctuations encountered in physical systems
is called a stationary Gaussian Markoff random process. Markoff processes
are random processes whose relation to the past does not extend beyond the
immediately preceding observation. As is shown in reference 2, page 215,
the autocorrelation function for this random process is given by

$$R_{\gamma\gamma} = \sigma_\gamma^2 e^{-\Lambda|T|} = \sigma_\gamma^2 e^{-\lambda|\tau|} \quad \text{where} \quad \sigma_\gamma^2 = R_{\gamma\gamma}(o) \equiv \langle \gamma^2 \rangle \tag{16}$$

The rate of fluctuation Λ and the time span T have been nondimensionalized
to be

$$\lambda = \Lambda d^2/v ; \quad \tau = Tv/d^2$$

The Fourier transform of $R_{\gamma\gamma}$ gives the power spectrum of the pressure fluctuations as a simple Lorenzian form:

$$S_{\gamma\gamma} = 2\lambda\sigma_{\gamma}^2/(\lambda^2 + \omega^2) \tag{17}$$

The σ_{γ}^2 is a dimensionless measure of the amplitude of the random fluctuations $\langle\gamma^2\rangle$. The larger the value of σ_{γ}^2, the larger the amplitude of the pressure fluctuations. The λ is a dimensionless measure of the average number of fluctuations per unit time. It can also be considered as the inverse of the dimensionless characteristic decay time of the autocorrelation. The larger the value of λ, the greater the fluctuation rate of the signal. The power of the pressure signal is given by the integral of the power spectrum over all frequencies. This can be written as

$$R_{\gamma\gamma}(o) = \int_{-\infty}^{+\infty} S_{\gamma\gamma}\ df = \sigma_{\gamma}^2 = \langle\gamma^2\rangle \tag{18}$$

The normalized power spectrum for the pressure gradient fluctuations $S_{\gamma\gamma}/\langle\gamma^2\rangle$ is plotted in figure 3 for different values of the rate of fluctuation parameter λ. It can be seen that for smaller values of λ much more of the spectral power is located in the lower frequencies since the frequency band for λ of 0.1 is much narrower than in the case for $\lambda = 100$.

Fluctuating Velocity Mean, Correlations, and Power Spectrums

The pressure-velocity cross correlation for the present case can be written using equations (11), (12), and (16) as

$$R_{\gamma v}(\tau) = \begin{cases} \sigma_{\gamma}^2 \displaystyle\sum_{k=1,3,5}^{\infty} \left[Y_K/(K^2 - \lambda)\right]\left[e^{-\lambda\tau} - \left[2\lambda/(\lambda + K^2)\right]e^{-K^2\tau}\right] & \text{for } \tau \geq 0 \\[2em] \sigma_{\gamma}^2 \displaystyle\sum_{k=1,3,5}^{\infty} Y_K e^{\lambda\tau}/(K^2 + \lambda) & \text{for } \tau < 0 \end{cases} \tag{19}$$

Also the cross spectrum can be written using equations (7), (13), and (17) as

$$S_{\gamma v}(\omega) = \left(\sum_{k=1,3,5}^{\infty} Y_K/(K^2 + i\omega) \right) 2\lambda\sigma_\gamma^2/(\lambda^2 + \omega^2) \qquad (20)$$

In a similar manner we can calculate the velocity autocorrelation from equations (11), (14), and (19) as

$$R_{vv}(\tau) = \sigma_\gamma^2 \sum_{k=1,3}^{\infty} \sum_{l=1,3}^{\infty} \left[Y_K Y_L/(L^2 - \lambda) \right] \left[e^{-\lambda\tau}/(\lambda + K^2) - \left(2\lambda/(\lambda + L^2) \right) e^{-L^2\tau}/(K^2 + L^2) \right] \qquad (21)$$

Similarly, we can write the velocity fluctuation power spectrum using equations (8), (15), and (17):

$$S_{vv}(\omega) = |H(\omega)|^2 S_{\gamma\gamma}(\omega) = \left(H_R^2 + H_I^2 \right) S_{\gamma\gamma} \qquad (22)$$

From equation (10) we can see that the ensemble average of the fluctuating velocity $\langle v \rangle$ at any given y is zero since the ensemble average of the fluctuating pressure gradient $\langle \gamma \rangle$ is zero.

The mean square velocity $\langle v^2 \rangle$ can be obtained from equation (21) since $R_{vv}(o,y) = \langle v^2 \rangle$. These results are shown in figure 4. Notice that the mean square velocity is equal to the total power of the velocity spectrum

$$R_{vv}(o,y) = \int_{-\infty}^{+\infty} S_{vv} \, df = \int_{-\infty}^{+\infty} |H(\omega)|^2 S_{\gamma\gamma}(\omega) df \qquad (23)$$

The spectral power or the mean square velocity is given by the product of the square of the gain factor times the pressure spectrum integrated overall frequency. From figure 2 we can see that the magnitude of the gain factor is smaller near the wall ($y = 0.1$) compared to the centerline ($y = 0.5$), so that the mean square velocity is smaller near the wall as compared to the

centerline. The mean square velocity goes to zero at the wall in figure 4, as would be expected from the zero wall velocity boundary condition. The gain factor in figure 2 is greatest at the lower frequency and has a high-frequency cutoff. Since the spectrum for the pressure gradient (fig. 3), is also greater at the lower frequencies for low values of λ as compared to the high λ case, the mean square velocity will be larger for the lower values of λ, as can be seen in figure 4.

The fluctuating velocity power spectrum given by equation (22) normalized by the total power of the spectrum at a given position in the channel $S_{vv}(y,f)/R_{vv}(y,o)$ is also shown in figure 3. These curves are discussed more fully later.

Power Dissipation Due to Velocity Fluctuations

It is desirable to know how much additional power must be supplied to the flow system to maintain the same average flow rate for the fluctuating flow as compared to the steady flow case. As shown in ref. (1), the external rate of work done by the pressure force w_e is equal to the sum of the rate of increase in kinetic energy K_e and the rate of dissipation of energy due to internal friction w_f. If we then take the ensemble average, the rate of change of the kinetic energy term will be zero because the process is stationary. We then have the external rate of work done by the pressure force w_e equal to the rate of dissipation of energy due to external friction w_f

$$-\langle \overline{U}P \rangle = \mu \int_0^1 \left\langle (\partial U/\partial Y)^2 \right\rangle dy \tag{24}$$

To find the rate of dissipation of energy due to internal friction we can then write

$$w_f = -\langle \overline{U}P \rangle = -\overline{U}_s P_s - \langle \overline{U}_t P_t \rangle = w_{f,s} - \langle \overline{U}_t P_t \rangle \tag{25}$$

If we let $w_{f,s}$ be the rate of dissipation due to steady flow, the ratio of increased dissipation due to the unsteady flow over the steady flow dissipation can be written as

$$\left(w_f - w_{f,s}\right)\big/w_{f,s} = \langle \overline{U}_t P_t \rangle / \overline{U}_s P_s = 12\langle \overline{v\gamma} \rangle = 12\overline{R}_{\gamma v}(o) \tag{26}$$

Integrating equation (19) over y and substituting into equation (26) give

$$\left(w_f - w_{f,s}\right)\big/w_{f,s} = 96\sigma_\gamma^2 \sum_{k=1,3,5}^\infty 1/K^2(K^2 + \lambda) \tag{27}$$

A plot of equation (27) is given in figure 5 as a function of the fluctuating rate parameter λ. As λ becomes very large, that is, fluctuations of the pressure gradient become very rapid, the frictional power loss reduces to the steady power loss. The frictional power loss increases with smaller values of λ or slower fluctuations of the pressure gradient.

Generation of Random Signal by Model Sampling

It would be helpful in certain cases to be able to generate a random signal analytically on the computer consistent with the power spectrum of the signal. This would be useful, for instance, in obtaining numerical solutions or various other statistical characteristics of linear or nonlinear equations of random systems that may be difficult to obtain by more usual analytical procedures. A method for generating random signals is given in reference 3. A somewhat different approach is used in the present analysis.

Discrete Fourier transforms. - When a waveform is to be analyzed on a digital computer, it is the discrete Fourier transform that must be used. This can be derived from the usual Fourier transform as shown in reference 2, page 56, as follows.

If $\gamma(t)$ is periodic in T_p, we can write the Fourier expansion

$$\gamma(t) = \sum_{n=-\infty}^{\infty} a_n e^{in2\pi t/T_p} \tag{28}$$

where

$$a_n = 1/T_p \int_{T_p/2}^{T_p/2} \gamma(t)e^{-i2\pi nt/T_p} \, dt \tag{29}$$

We can see from equation (28) that

$$\lim_{T_p \to \infty}(T_p a_n) = \gamma_\omega \tag{30}$$

Similarly, if γ_ω is periodic in f_p, we can write

$$\gamma_\omega = \sum_{n=-\infty}^{\infty} d_n e^{-i2\pi nf/f_p} \tag{31}$$

where

$$d_n = (1/f_p) \int_{-f_p/2}^{f_p/2} \gamma_\omega e^{i2\pi f/f_p} \, df \tag{32}$$

We can see that, similarly,

$$\lim_{f_p \to \infty}(f_p d_n) = \gamma(t) \tag{33}$$

If we take the time between sample values of γ_k as Δt, we can take

N samples so that $N \Delta t = T_p$. Then, assuming that $\Delta t = 1/f_p$ we can

write equation (28) as

$$\gamma_k(k \, \Delta t) = \sum_{n=-N/2}^{N/2} a_n e^{i2\pi kn/N} \tag{34}$$

We can also write equation (31), assuming that $N \Delta f = f_p$, as

$$a_n = (1/N) \sum_{k=-N/2}^{N/2} \gamma_k e^{-i2\pi kn/N} \qquad (35)$$

Since a_n can be related to the Fourier transform γ_ω by equation (30), equations (34) and (38) form a discrete Fourier transform pair that is an approximation of the Fourier integral transform pair.

A numerical method for evaluating either equation (34) or (35) in a very efficient manner on digital computers has been developed called the fast Fourier transform (ref. 4). One implementation of the fast Fourier transform is available as an IBM-scientific subroutine package called HARM/DHARM. Many others are also available.

<u>Gaussian random process</u>. - Since γ_k is a real function $a_{n,R}$ must be an even function and $a_{n,I}$ must be an odd function around $n = 0$. Then we can write

$$\gamma_k = \sum_{n=-N/2}^{N/2} a_{n,R} \cos(2\pi nk/N) - a_{n,I} \sin(2\pi nk/N) \qquad (36)$$

We can assume a Gaussian random process for γ_k. This process is commonly used as an idealization of many natural phenomena associated with the super-position of a large number of many small effects. It is shown in reference 5, page 160, that for a Gaussian random process the following conditions are true: a is a random variable with a Gaussian distribution also

$$\langle a_{n,R} a_{k,R} \rangle = \langle a_{n,I} a_{k,I} \rangle = \begin{cases} \langle a_n^2 \rangle & k=n \\ 0 & k \neq n \end{cases} : \quad \langle a_n b_k \rangle = 0 \qquad (37;38)$$

Then, spectrum of $\gamma(t)$ can be shown to be related to $\langle a_n^2 \rangle$ by

$$S_{\gamma\gamma}\big|_{\omega=n2\pi/T_p} = 2T_p\left\langle a_n^2\right\rangle \qquad \text{when} \qquad n \neq 0 \tag{39a}$$

$$S_{\gamma\gamma}\big|_{\omega=0} = T_p\left\langle a_o^2\right\rangle \qquad \text{when} \qquad n = 0 \tag{39b}$$

Model sampling to generate signal. - To generate a random signal $\gamma(t)$ we can use equation (34) and the fast Fourier transform program. The terms $a_{n,R}$ and $a_{n,I}$ are random variables randomly picked from the joint Gassian distribution

$$\bar{f}(a_{n,R}a_{n,I}) = \left(1/2\pi\left\langle a_n^2\right\rangle\right)e^{-\left(a_{n,R}^2+a_{n,I}^2\right)/2\left\langle a_n^2\right\rangle} \tag{40}$$

Following the method given in reference 6, page 39, we can randomly choose values of $a_{n,R}$ and $a_{n,I}$ that will satisfy the distribution of equation (40) by using the following equations:

$$a_{n,R} = \left(2\left\langle a_n^2\right\rangle\right)^{1/2}\left(-\ln R_r\right)^{1/2}\cos 2\pi R_\theta \tag{41a}$$

$$a_{n,I} = \left(2\left\langle a_n^2\right\rangle\right)^{1/2}\left(-\ln R_r\right)^{1/2}\sin 2\pi R_\theta \tag{41b}$$

where R_θ and R_r are two different random numbers randomly picked from a uniform distribution between 0 and 1. The values of R can readily be generated by the computer. The values of $\left\langle a_n^2\right\rangle$ can be obtained from equation (39) using the appropriate power spectrum $S_{\gamma\gamma}$. Recalling that $a_{n,R}$ is an even function and $a_{n,I}$ is an odd function, in the particular fast Fourier program available (HARM/DHARM), we only need find $a_{n,R}$ and $a_{n,I}$ from $n = 0$ to $N/2$. Then $a_{(N/2)+1,R} = a_{(N/2)-1,R}$, etc. Similarly, for $a_{n,I}$ values were only needed for $n = 0$ to $n = N/2$; since $a_{(N/2)+1,I}$ equaled $-a_{(N/2)-1,I}$, etc., $a_{o,I}$ was equal to zero.

Pressure Gradient Signal Results

The normalized fluctuating pressure gradient $\gamma/\langle\gamma^2\rangle^{1/2}$ is shown in figure 6 for different values of λ. The pressure gradient power spectrum used in obtaining these results was assumed to be a stationary Gaussian Markoff process and is given by equation (17) and plotted in figure 3. The results were calculated for values of N of 128 and λT_p taken as 100.

The curves were computer plotted by joining the output points by dotted lines. Since the spectrum for the higher fluctuating rate parameter $\lambda = 100$ is greater at the higher frequencies, as can be seen in figure 3, the resulting pressure signal for large λ has many more fluctuations and crossing of the 0 value line per unit time than is the case for the lower values of λ.

Generating Velocity Signal From Pressure Signal

The method of calculating the velocity signal from the pressure signal is as follows. We can write, similar to equation (36),

$$v_k = \sum_{n=-\infty}^{\infty} (b_{n,R} \cos 2\pi nk/N + b_{n,I} \sin 2\pi nk/N) \tag{42}$$

where $b_{n,R}$ is an even function and $b_{n,I}$ is an odd function. From equations (6) and (30) we can write

$$v_\omega = b_n T_p = \left(H\big|_{\omega=n2\pi/T_p}\right)\left(a_n T_p\right)$$

or

$$b_n = H_n a_n \tag{43}$$

Thus, by finding the values of a_n for a given signal γ_t, as discussed previously, we can use equation (43) to obtain the new values b_n which can be used in equation (42) to obtain the the velocity signal v using the fast Fourier transform program.

We can see from equation (43) that the mean values of $b_{n,R}$ and $b_{n,I}$ are zero. Also, since $a_{n,R}$ and $a_{n,I}$ are normally distributed, $b_{n,R}$ and $b_{n,I}$ are also normally distributed. The variance of b_n can be seen to be

$$\left\langle b^2_{n,R} \right\rangle = \left\langle b^2_{n,I} \right\rangle = \left\langle a^2_n \right\rangle \left(H^2_{n,R} + H^2_{n,I} \right) = \left\langle a^2_n \right\rangle \left| H_n \right|^2 \qquad (44)$$

except at $n = 0$

$$\left. \left\langle b^2_{n,I} \right\rangle \right|_{n=0} = 0 \\ \left\langle b^2_{o,R} \right\rangle = \left\langle a^2_{o,R} \right\rangle H^2_{o,R} \qquad \qquad (45)$$

The spectrum in this case would be given as in equation (39) by

$$S_{vv}(n) = T_p 2 \left\langle b^2_n \right\rangle = T_p 2 \left\langle a^2_n \right\rangle \left| H \right|^2 = S_{\gamma\gamma}(n) \left| H_n \right|^2 \qquad (46)$$

except at $n = 0$ when

$$S_{vv}(o) = T_p \left\langle b^2_o \right\rangle = S_{\gamma\gamma}(o) \left| H_o \right|^2 \qquad (47)$$

This shows that $b_{n,R}$ and $b_{n,I}$ cannot only be found from a_n but can be picked directly from a normal distribution with a variance of b^2_n given by equation (46) as in the case of a_n values.

In figure 6 the normalized fluctuating velocity at the centerline of the channel $v_{y=0.5} \big/ \left(\left\langle v^2 \right\rangle^{1/2} \right)_{y=0.5}$ is plotted as solid lines. These results were calculated from equation (42) using the fast Fourier transform routine. The coefficients b_n were found from equation (43), which gives the values in terms of a_n which are the coefficients of the random pressure fluctuations. These were randomly chosen by equation (41). Thus, the velocity shown by the solid line on each graph is caused by the pressure fluctuation shown as the dotted line on the same graph. Notice that all the curves have been normalized by their own root mean square values.

For low values of λ, the shapes of the curves are very similar but there is a small time lag in the velocity curve compared to the pressure curve. This time lag can be explained by postulating a distortionless frequency response function H' with a distortionless gain factor $|H(\omega)| = |H|'$ and a distortionless phase factor $\varphi' = -\omega t_0$.

Then equation (6) can be written as

$$V_\omega = |H|'e^{i\omega t_0} \Upsilon_\omega \tag{48}$$

Taking the inverse transform and using the time shifting theorem gives

$$V(t) = |H|'\Upsilon(t + t_0) \tag{49}$$

This shows, for the distortionless response function, the velocity signal lags the pressure signal by a time increment t_0, while the amplitude is changed by an amount $|H|'$.

In comparing the distortionless frequency response function to the present response function we can see from figure 2 that for small angular frequencies the response function approaches the distortionless case. We can calculate the time lag t_0 for small angular frequencies by solving for φ as $\omega \to 0$. This gives, from equation (9), $\varphi_{\omega \to 0} = -\omega(0.0781)$. Thus, the time lag between the velocity and pressure signals for small ω is given by $t_0 = 0.0781$. Thus, in figure 6 for $\lambda = 1$ we see the velocity signal is close to the pressure signal with a small time lag between them. This is because the response function is close to distortionless for small ω and the pressure signal for small λ is concentrated in the small ω region (see fig. 3).

For the higher values of λ we can see that the velocity signal does not contain many of the higher frequency fluctuations that are present in the

velocity signal. This is because the gain factor (see fig. 3) has a high-frequency cutoff which caused the velocity spectrum to have a similar high-frequency cutoff. Since at high λ much of the pressure spectrum is in the higher frequencies, these higher frequencies are not transmitted to the velocity signal.

In figure 7, the velocity signal at a given position y in the channel, normalized by its root mean square value at the same y value, is plotted at two different values of y for the same pressure signal. For low values of λ the curves near the center of the channel ($y = 0.5$) are very similar to that nearer the wall ($y = 0.01$). This happens because the transfer function for small ω is close to distortionless. The velocity signals near the wall, although of a smaller amplitude than the velocity signal near the center of the channel (see normalizing factor in fig. 4), both have almost identical shapes. At the higher values of λ we see that the centerline signal fluctuates much less than the velocity signal near the wall. This is due to the fact that the gain factors for y close to the wall are flatter and do not have as strong a high-frequency cutoff as the gain factors near the center. This causes the velocity spectrum near the wall ($y = 0.1$) given in figure 3 to be flatter and extend to higher frequencies than the velocity spectrum near the center of the channel.

At the higher values of λ, we can also notice a time lag between the signals. This effect is due to the phase factor shown in figure 2. It can be seen that the phase factor curves for the signals closer to the wall have smaller slopes and so have a smaller delay time than the velocity near the center of the channel.

RESULTS AND CONCLUSIONS

The effect of superimposing a randomly fluctuating pressure gradient of a stationary Gaussian Markovian form with a zero mean value upon a steady pressure gradient will cause a randomly fluctuating velocity component to be superimposed over the steady flow in a channel. The mean value of the velocity fluctuation is zero. The mean square value of the velocity fluctuations which is a measure of the amplitude of the fluctuations will be highest in the center of the channel and reduce to zero at the wall. Also, the slower the rate of the pressure fluctuations, the greater the amplitude of the velocity fluctuations.

The frictional power loss in pumping the fluid is increased by the pressure fluctuations, the slower pressure fluctuations giving larger power losses.

The normalized velocity signal values were very similar to the normalized pressure signal but with a dimensionless time lag t_0 of about 0.0781 for low pressure fluctuation rates. At the higher pressure fluctuation rates the higher frequencies of the pressure signal did not appear in the velocity signal.

Comparison of the velocity signals across the channel normalized by its local root mean square value showed that for low fluctuation rates in the pressure signal the values of the normalized velocity near the wall were almost identical to the normalized velocities near the center of the channel. However, at the higher pressure fluctuation rates the higher frequency fluctuations present in the velocities near the wall do not appear in the velocities near the center of the channel, and the velocities near the center of the channel lag the velocities near the wall.

The random pressure signal function was generated by a Fourier series expansion where the coefficients were randomly chosen by model sampling from

a frequency distribution whose parameters are given by the power spectrum of the signal. By use of the fast Fourier transform method of computation the function can be rapidly evaluated from its Fourier coefficients. The Fourier expansion of the fluctuating pressure signal can then be used to calculate the randomly varying velocity at various positions from the wall. These velocity results can be useful when the details of a randomly fluctuating velocity distribution in a channel are needed, as for instance in convective heat-transfer problems.

<div align="center">ACKNOWLEDGEMENT</div>

REFERENCES

[1] Siegel R., and Perlmutter, M., "Heat Transfer for Pulsating Laminar Duct Flow," Journal of Heat Transfer, Vol. 84, No. 2, May 1962, pp. 111-123.

[2] Bendat, J. S., Principals and Applications of Random Noise Theory, John Wiley & Sons, Inc., 1958.

[3] Broste, N. A., "Digital Generation of Random Sequences with Specified Autocorrelations and Probability Density Functions," Rep. RE-TR-70-5, Mar. 6, 1970, Army Missile Command. (Available from DDC as AD-704702.)

[4] Cochran, W. T., Cooley, J. W., Favin, D. L., Helms, H. D., Kaenel, R. A., Lang, W. W., Maling, G. C., Jr., Nelson, D. E., Rader, C. M., and Welch, P. D., "What is the Fast Fourier Transform?," Proceedings IEEE, Vol. 55, No. 10, Oct. 1967, pp. 1664-1674.

[5] Laning, J. H., Jr., and Battin, R. H., Random Processes in Automatic Control, McGraw-Hill Book Co., Inc., 1956.

[6] Hammersley, J. M., and Handscomb, D. C., Monte Carlo Methods, John Wiley & Sons, Inc., 1964.
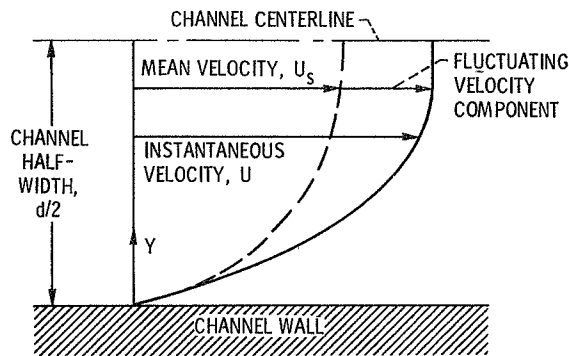
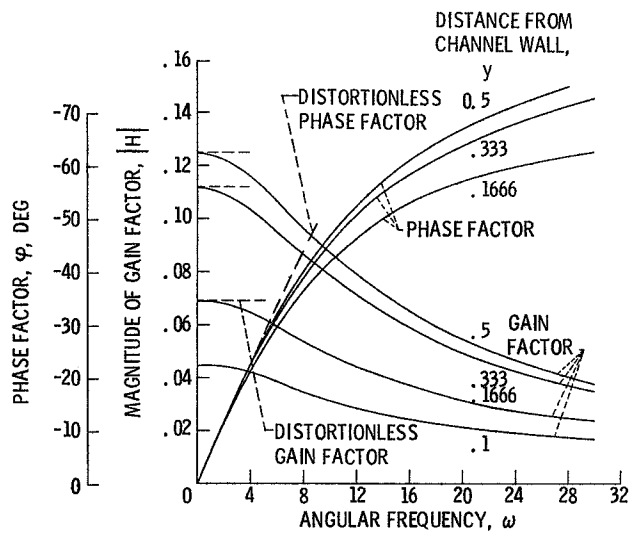Figure 1. - Parallel plate channel flow model.

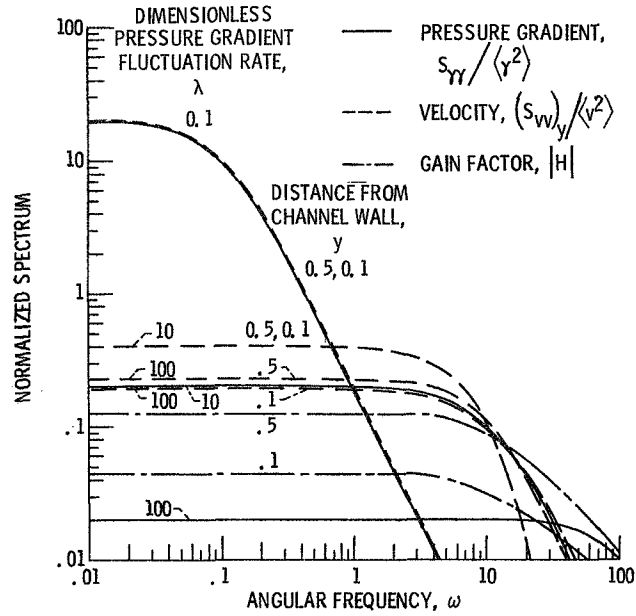Figure 2. - Frequency response function of system.

Figure 3. – Normalized spectrums.
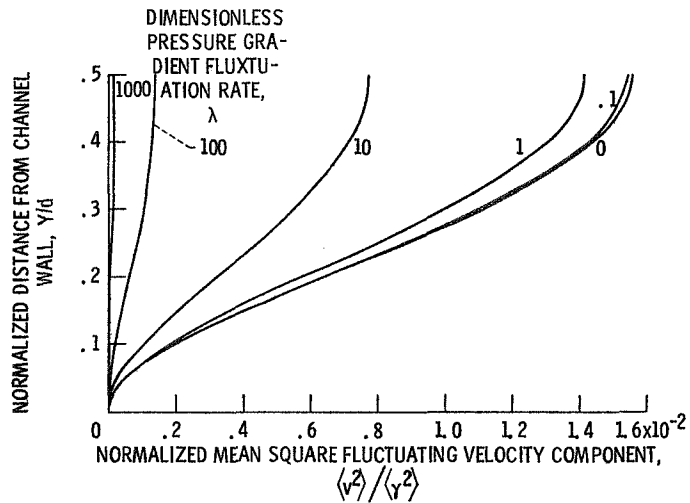

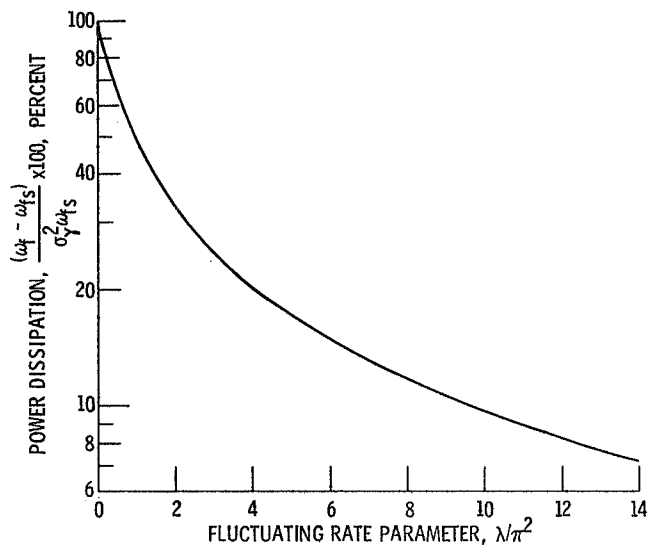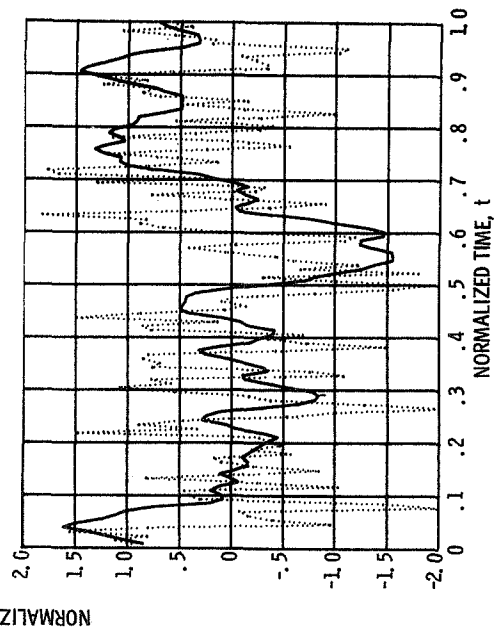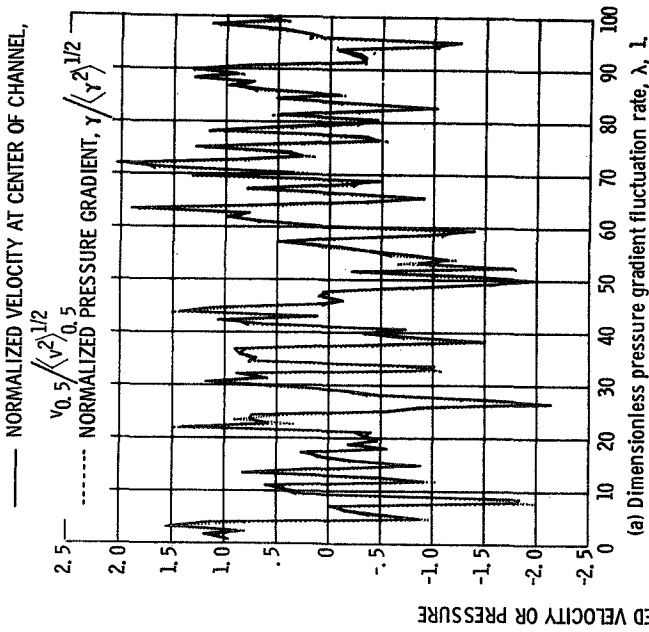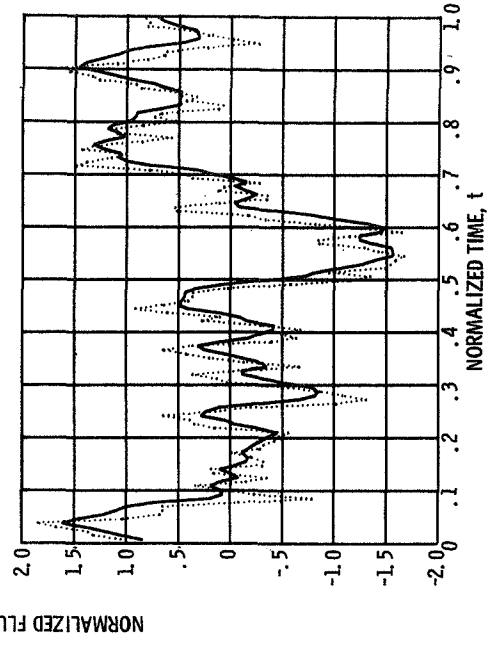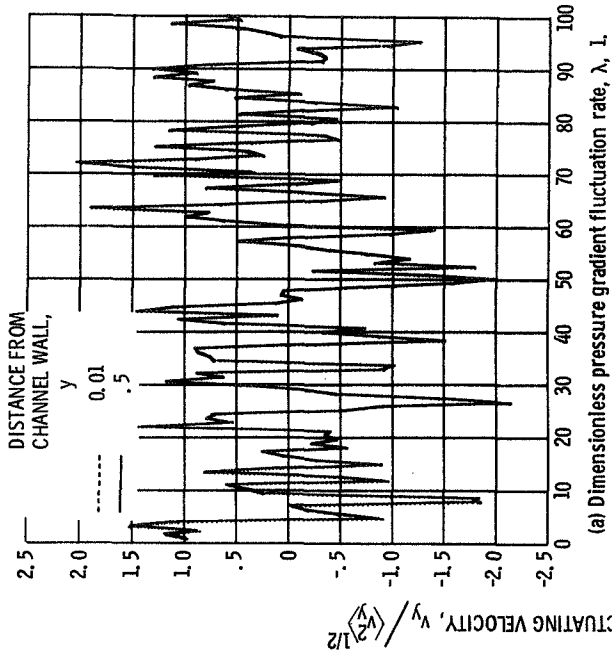Figure 4. – Normalized mean square fluctuating velocity component across channel.

Figure 5. - Percentage increase in power dissipation ratio due to flow fluctuations.

(a) Dimensionless pressure gradient fluctuation rate, λ, 1.

(b) Dimensionless pressure gradient fluctuation rate, λ, 100.

Figure 7. - Fluctuating velocity signals at different positions in channel normalized by their local root mean square value.

DISTANCE FROM CHANNEL WALL, y

0.01
.5

NORMALIZED FLUCTUATING VELOCITY, $v_y / \langle v_y^2 \rangle^{1/2}$

NORMALIZED VELOCITY AT CENTER OF CHANNEL, $v_{0.5} / \langle v^2 \rangle^{1/2}_{0.5}$

NORMALIZED PRESSURE GRADIENT, $\gamma / \langle \gamma^2 \rangle^{1/2}$

(a) Dimensionless pressure gradient fluctuation rate, λ, 1.

(b) Dimensionless pressure gradient fluctuation rate, λ, 100.

NORMALIZED TIME, t

Figure 6. - Normalized fluctuating pressure gradient and velocity signal. Distance from channel wall, y, 0.5.

NORMALIZED VELOCITY OR PRESSURE